Journal of Nano- and Electronic Physics
Vol. **13** No 4, 04016(6pp) (2021)

Журнал нано- та електронної фізики
Том **13** № 4, 04016(6cc) (2021)

Annealing Effects on the Optoelectronic Performance of Au and CuO Nanoparticles Incorporated P3HT/PCBM Solar Cells

Aruna P. Wanninayake

Department of Physics and Electronics, University of Kelaniya, Kelaniya, Sri Lanka

(Received 09 March 2021; revised manuscript received 03 August 2021; published online 20 August 2021)

Sun energy conversion to electrical energy using nanostructured organic/inorganic hybrid semiconductors is one of the best solutions for today's energy crisis. In particular, researchers are focusing on multi-techniques to increase the power conversion efficiency of polymer solar cells, including thermal annealing and the incorporation of metal or transition metal oxide nanoparticles (NPs) into the active layer of polymer solar cells (PSCs). The design approaches for thermal annealing are to improve the nanoscale morphology and optical properties of the active layer. The incorporation of metal NPs is based on localized surface plasmonic resonance (LSPR) effect which can be used to enhance the optical absorption in photovoltaic devices. Meanwhile, transition metal oxide NPs such as copper oxide (CuO) NPs in the active layer play a key role as light harvesting centers, charged particle hopping centers, and surface morphology developer, enabling a considerable reduction in the physical thickness of solar photovoltaic absorber layers. In this study, thermal annealing was used to optimize the power conversion efficiency of bulk heterojunction P3HT/PC70BM SCs synthesized by incorporating gold nanoparticles and copper oxide nanoparticles. Thermal annealing increased the power conversion efficiency by up to 48.3 % compared to the reference cell. The optimum short-circuit current (J_{sc}) of the cells was measured to be 8.704 mA/cm^2 compared to 5.838 mA/cm^2 in the reference cell; meanwhile, the external quantum efficiency (EQE) increased from 44 to 64 %.

Keywords: Plasmonic effect, Thermal annealing, PSCs, P3HT, PCBM, PCE.

DOI: 10.21272/jnep.13(4).04016 PACS numbers: 84.60.Jt, 85.60.Bt

1. INTRODUCTION

Polymer solar cells (PSCs) are considered as the third-generation solar cells having many advantages such as light weight, flexibility, relatively low cost, easy fabrication and so on [1-4]. In recent years, much effort has been made to develop PSCs and increase the power conversion efficiency (PCE) of single-junction and tandem solar cells. The PCE has exceeded 14 % [5-7] and 17 % [8] of single-junction and tandem solar cells, respectively. These improvements are the result of the tuning of active layer materials, the development of the surface morphology of thin films, reducing the series and shunt resistances of devices, etc. A blend of Regioregular poly(3-hexylthiophene) (P3HT) and [6,6]-phenyl-C61-bu-tyric acid methyl ester (PCBM) is one of the common and promising materials for achieving high PCE because of the high self-organizing ability [9, 10], high hole mobility, and a broad absorption range in the red region of the electromagnetic spectrum.

Many researchers have demonstrated different independent approaches to improve the PCE of PSCs which consist of P3HT and PCBM as active layer materials. Some of the above approaches include metal/metal oxide nanoparticles (NPs) incorporated in the active layer or the hole transport layer [11], thermal annealing [12], and slow growth of the active layer by controlling the solvent evaporation rate. The slowly grown active layer is a new approach which reduces the series resistance of the device and improves optical absorption.

Illuminated metal NPs such as Au and other metallic nanostructures can be used to increase light absorption of polymer thin films due to the localized surface plasmon resonance (LSPR) effect, which can significantly enhance local electromagnetic fields [13, 14]. The LSPR of metallic NPs is referred to as the collective oscillation of electrons located on metallic NPs, which are excited by incident photons at the resonant frequency [15]. The LSPR excitation of metallic NPs results in improved electromagnetic fields, light absorption and scattering due to their physical and elemental parameters, which leads to enhanced device performance. Brown et al. [16] showed that metallic nano-structures in the active layer can scatter incident photons along a long propagation path, resulting in higher light absorption and photocurrent generation in PSCs. Lu et al. [17] reported a 20 % enhancement of PCE of Au and Ag incorporated PSCs due to the LSPR effect. On the other hand, NPs of transition metal oxides, such as copper oxide nanoparticles (CuO NPs), have gained special attention due to their low cost, non-toxicity, and high optical absorption capabilities. CuO is a *p*-type semiconductor with a direct band gap energy of 1.5 eV which is close to the ideal energy gap of 1.4 eV for the manufacture of solar cells with high optical absorbing [18-20]. In a previously reported work by the author, it is shown that the incorporation of CuO NPs in the active layer increases the PCE of solar cells by 40.6 %.

Thermal annealing is a very important method for improving the crystallinity of P3HT molecules, and therefore, the molecular orientation and morphology of films. Subsequent annealing of the devices encourages aggregation of PCBM, forming continuous pathways in the P3HT/PCBM active layer, and improves efficient charge separation and transport. Furthermore, crystallinity of the structure, molecular orientation, and morphology of the films strongly correlate with the charge transfer process in organic semiconductor thin films. Li et al. [21] and Wang et al. [22] reported, respectively, an

increase in the PCE of 0.292 % and 4 % by thermal annealing method. Park et al. [23] demonstrated that thermal annealing affects the morphological changes of P3HT thin films and hence enhances the PCE.

In this work, P3HT/PCBM based solar cells were fabricated containing Au and CuO NPs in the active layer. Also, the annealing effect on P3HT/PCBM/Au/CuO NPs devices will be demonstrated through the nanoscale morphology aspect and reveal its influence on the PCE of the solar cells.

2. EXPERIMENTAL METHODS

2.1 Materials

Poly(3-hexylthiophene) (P3HT) (Rieke Metals), phenyl-C70-butyric acid methyl ester (PC70BM) (SES Research), NPs of gold (Au) (15 nm diameter) and NPs of CuO (10-30 nm diameter) (nanocs.com), glass substrates with a size of 24 × 80 × 1.2 mm (12 Ω/cm^2) with an Indium Tin Oxide (ITO) conductive layer of 25-100 nm (nanocs.com) and aluminium coils with a diameter of 0.15 mm (Ted-Pella, Inc.) were used as received. Poly(3,4 ethylenedioxythiophene)-poly(styrenesulfonate) (PEDOT/PSS) was obtained from Sigma Aldrich and mixed with an equal amount of distilled water. All processing and characterization work of the PSC devices was conducted under same experimental conditions.

2.2 Device Fabrication

Conductive glass substrates were successively ultrasonically cleaned with ammonium hydroxide, hydrogen peroxide, distilled water, methyl alcohol, and isopropyl alcohol. The fabrication of polymer-based solar cells containing Au NPs was carried out in a N_2 filled glove box. The P3HT-PC70BM blend was obtained by diluting equal amounts of regioregular P3HT and PC70BM (10 mg each) with 2 ml of chlorobenzene (C6H5Cl) and mixing for 14 h at 50 °C. 0.05 mg of Au NPs (15 nm diameter) and 0.6 mg of CuO NPs (10-30 nm diameter) were added to the mixture, so that the weight ratio of P3HT/PCBM/Au NPs/CuO NPs in the final blends was 10:10:0.05:0.6.

The solar cell devices were spin coated in a glove box with N_2 atmosphere. A 40 nm thick PEDOT/PSS layer, which serves as a thin hole-transport layer, was spin coated at a rotational velocity of 4000 rpm, followed by heating at 120 °C for 20 min in air. When the temperature of the samples reached the ambient temperature, the P3HT:PC70BM:(0.05 mg) Au NPs:(0.6 mg) CuO NPs solution was spin coated for 2 min at 1000 rpm. The active layers had an average thickness of 120 nm and a surface area of 0.12 cm^2. A schematic illustration of the layered structure of the fabricated devices is shown in Fig. 1. All the fabricated devices were annealed at 150, 200 and 250 °C for 30 min. A series of solar cell devices were tested under the same experimental conditions.

2.3 Characterization

The current density-voltage (*J-V*) characterization was carried out for all PSCs using a UV solar simulator with an AM 1.5G filter and a lamp intensity of 100 mW/cm^2. A source meter (Keithley 2400) was used to obtain the *J-V* measurements. Device parameters such as short-circuit current (J_{sc}), open-circuit voltage (V_{oc}), fill factor (FF) and power conversion efficiency (PCE) were recorded under ambient conditions. A quantum efficiency measurement kit (Newport-425) embedded in the solar cell simulator was used to obtain external quantum efficiency (EQE) values. A PerkinElmer LAMBDA 650 spectrophotometer was used to obtain the optical properties of the cells. The crystallinity studies of the thin layers were performed by XRD with a Cu/K source at a rate of 0.2° per minute. The recorded range of the X-ray spectra was 4-7°. An Agilent 5420 atomic force microscope (AFM) was used to analyze the surface morphology. The Pico Image Basics and Gwyddion software were utilized to determine the root mean square (RMS) roughness (σ_{rms}) of the surface under ACAFM non-contact mode with set point 1.60, I-gain of 10 and scanned area of 2 × 2 μm. The layer structures of the fabricated solar cells were analyzed using a scanning electron microscope with an energy dispersive X-ray detector (FEG-SEM Hitachi S-4800).

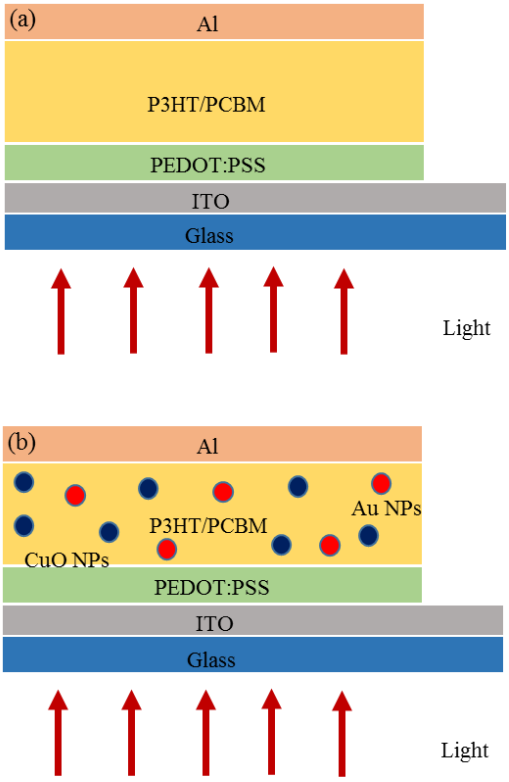

Fig. 1 – Schematic illustration of Au and CuO NPs incorporated PSCs

3. RESULTS AND DISCUSSION

The observation of the surface morphology of the active layer reveals the reorganization of P3HT nanoclusters in the structure under different annealing temperatures. Fig. 2 depicts the AFM images of P3HT/PCBM/Au/CuO NPs thin films before and after thermal annealing. For P3HT/PCBM/Au/CuO NPs thin films before thermal annealing, the surface was relatively smooth with an RMS roughness of 0.90 nm. However, after thermal annealing treatment at 150, 200 and 250 °C for 30 min, the RMS roughness values increased to 1.10,

1.41 and 1.52 nm, respectively. This increased roughness will lead to an increase in the interfacial contact area, facilitating high charge collection at the electrodes. With increasing annealing temperature, P3HT/PCBM phase separation is encouraged and P3HT molecules can be restructured as small crystallites in the thin film. Also, this increased surface roughness of cells with Au and CuO NPs provides evidence of adequate space for P3HT crystallites to form the active layer structure.

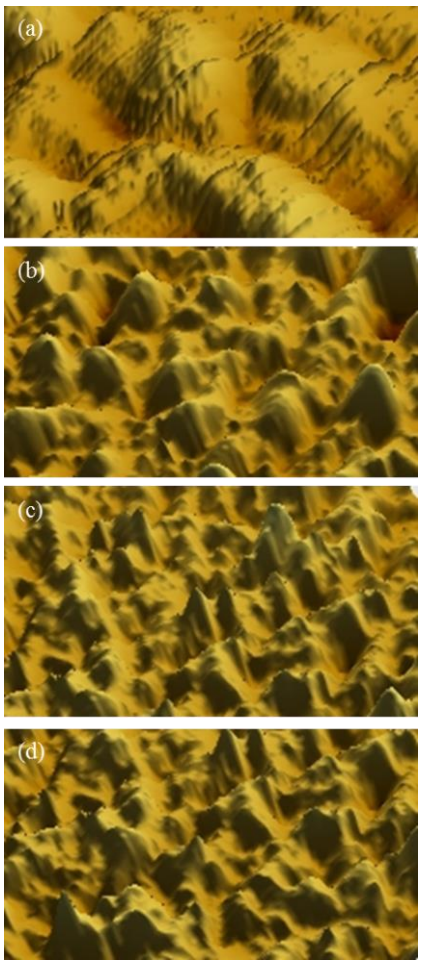

Fig. 2 – AFM images of the blended films at various annealing temperatures: (a) as-cast film, (b) 150 °C, (c) 200 °C, (d) 250 °C

SEM images of the hybrid structure of the fabricated PEDOT:PSS/P3HT:PCBM/Au/CuO NPs device before and after thermal annealing are shown in Fig. 3. The P3HT/PCBM active layer with embedded Au and CuO NPs had a thickness of about 100-160 nm. This helps to minimize the charge recombination losses in devices. The thickness of the PEDOT:PSS hole transport layer was estimated as 40 nm.

With annealing treatment at different temperatures, the P3HT molecules are well dispersed in the thin film, forming charge hopping pathways for electrons and holes to transport. Amorphous PCBM molecules are surrounded by P3HT molecules disabling the continuous pathways for charge transport in the thin film. Hence, the photogenerated holes and electrons can be recombined before transporting to the electrodes. Therefore, the charge hopping process is one of the crucial factors for smooth charge transfer.

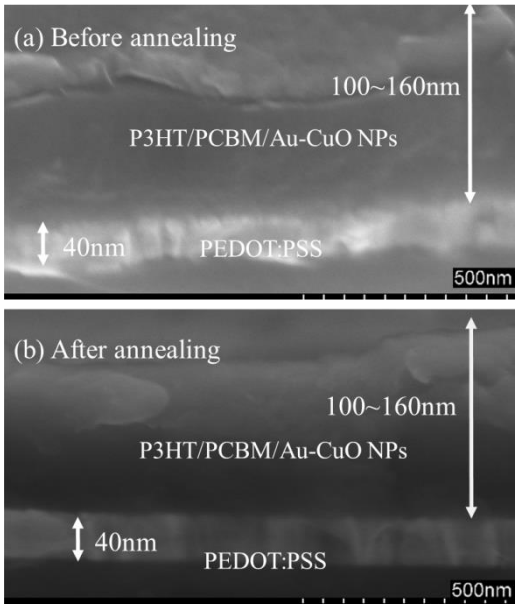

Fig. 3 – SEM images of the P3HT/PCBM/Au/CuO NPs hybrid PSCs: (a) before annealing, (b) after annealing at 200 °C

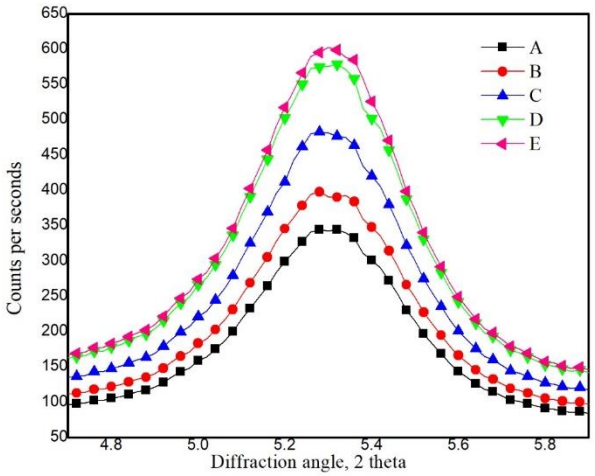

Fig. 4 – XRD spectra for Au and CuO NPs incorporated P3HT/PCBM thin films before and after annealing: (A) without annealing and no NPs, (B) without annealing and with 0.05 mg Au NPs + 0.6 mg CuO NPs, (C) with 0.05 mg Au NPs + 0.6 mg CuO NPs and annealing at 150 °C, (D) with 0.05 mg Au NPs + 0.6 mg CuO NPs and annealing at 200 °C, (E) with 0.05 mg Au NPs + 0.6 mg CuO NPs and annealing at 250 °C

Formation of P3HT crystals with annealing at higher temperatures will be a solution for charge particles to hop from one crystal to the neighboring crystal creating better charge transfer. Fig. 4 depicts the XRD spectra of active layers that have structurally changed due to high-temperature annealing treatment. These XRD spectra were obtained from 4 to 7° at a rate of 0.2° per minute using automatic slits. The intensity increased with increasing annealing temperature in the peak at 200 °C for all P3HT:PC70BM:Au:CuO NPs layers that corresponds to the enhanced crystallinity of P3HT molecules. It is clear that the X-ray data shows the increase in the crystallinity of P3HT main chains in the blend. On the other hand, addition of Au and CuO NPs has also improved the intensity of XRD peaks (B) which implies the

enhanced crystallinity. This may be due to the encouraged P3HT and PCBM phase separation with Au and CuO NPs. It is important to note that the results obtained from the XRD peaks show a similar trend to the data obtained from the AFM images.

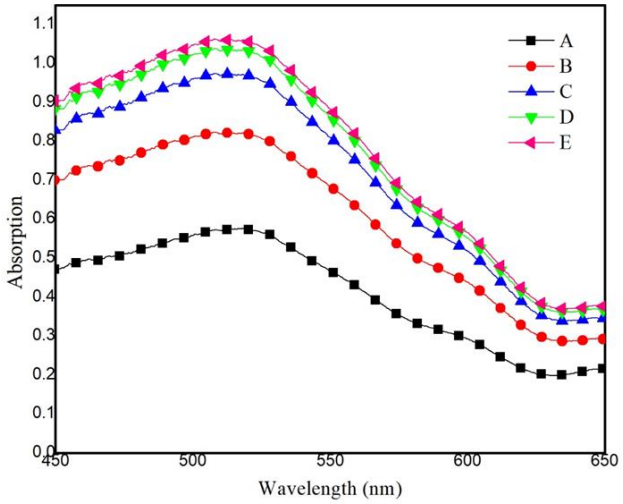

Fig. 5 – Optical absorption spectra of hybrid solar cells: (A) without annealing and no NPs, (B) without annealing and with 0.05 mg Au NPs + 0.6 mg CuO NPs, (C) with 0.05 mg Au NPs + 0.6 mg CuO NPs and annealing at 150 °C, (D) with 0.05 mg Au NPs + 0.6 mg CuO NPs and annealing at 200 °C, (E) with 0.05 mg Au NPs + 0.6 mg CuO NPs and annealing at 250 °C

The optical absorption spectra were recoded to examine the collective optical absorption effects raised from Au and CuO NPs in the P3HT/PCBM thin film. Relevant UV-Vis measurements of ITO/PEDOT:PSS/P3HT:PCBM:Au:CuO NPs were performed as shown in Fig. 5. These optical absorption measurements can be a result of the plasmonic effect due to Au NPs and enhanced crystallinity due to thermal annealing and CuO NPs [11, 19]. The NPs give an enhanced single peak compared to the reference cell in the visible range at 450-550 nm wavelength based on the shape, size, density, and surrounding NPs [19]. Generally, smaller Au NPs exhibit a dipolar pattern of a uniform field in all directions due to optical absorption compared to forward and backward scattering by larger Au NPs. Also, the absorption spectra of Au NPs embedded in polymer thin films clearly show evidence of the LSPR effect due to Au NPs. The optical absorption spectra depict that Au NPs contribute to the peak absorption resonances at a wavelength of 525 nm which leads to the π^*-π transitions. On the other hand, a significant increase in the P3HT crystallinity, upon the addition of CuO NPs can be attributed to the self-assembly of conjugated P3HT chains, leading to ordered formation in the blend. This enhanced crystallinity due to the addition of CuO NPs and thermal annealing significantly contributes to an increase in optical absorption in thin films. The spectral diagrams of optical absorption after annealing at 150, 200 and 250 °C show significant improvements due to the enhanced P3HT crystallinity. The photon absorption efficiency determines the photon absorption capacity of the solar cells. Light absorption of a semiconductor thin film is controlled by the energy band structure, absorption coefficient, and the thickness of the photoactive layer. According to the spectral diagrams, the optical absorption of P3HT/PCBM solar cells was improved after incorporating CuO and Au NPs in the devices and thermal annealing.

Absorption of a photon with an energy greater than the E_g value (1.99 eV) for P3HT generates an exciton which diffuses to the P3HT/PCBM interface. The E_g value of CuO NPs incorporated P3HT/PCBM was calculated using Tuac formula: $(ahv)^m = B(hv - E_g)$, where hv is the energy of incident photons in eV, $m = 1/2$ for indirect and 2 for direct allowed transitions, B is a constant related to the material, h is the Plank's constant, v is the frequency of the photon, E_g is the optical band gap in eV [24]. Assuming direct transitions between the valence band and the conduction band, E_g can be determined by the plot of $(ahv)^2$ versus (hv) at $a = 0$. The estimated E_g value for CuO NPs is approximately 2.14 eV. The estimated E_g value of the P3HT/PCBM blend was 2.71 eV. After incorporating CuO NPs into the P3HT/PCBM blend, the E_g value was 2.64 eV. However, the E_g value did not change significantly with the addition of Au NPs together with CuO NPs in the blend. The E_g value of the solar cell annealed at 200 °C was 2.58 eV. This reduced band gap facilitated a smooth transition of free electrons from the donor material to the acceptor material.

The EQE of a photovoltaic device is the ratio between the incident photons and the free charge carriers generated by the device. Therefore, the EQE spectra of different sets of solar cells were obtained for better understanding of the enhanced J_{sc} in the fabricated devices. The EQE spectra of the devices are shown in Fig. 6. After Au and CuO NPs were incorporated into the devices, the relevant EQE spectra proportionally enhanced in the wavelength range from 410 to 550 nm. Furthermore, the EQE spectra were slightly increased in the same wavelength range after annealing at temperature values of 150, 200 and 250 °C, and the peak EQE values were 60, 64 and 61 %, respectively. However, the optimum EQE spectrum was obtained from the devices annealed at 200 °C, and the peak EQE value

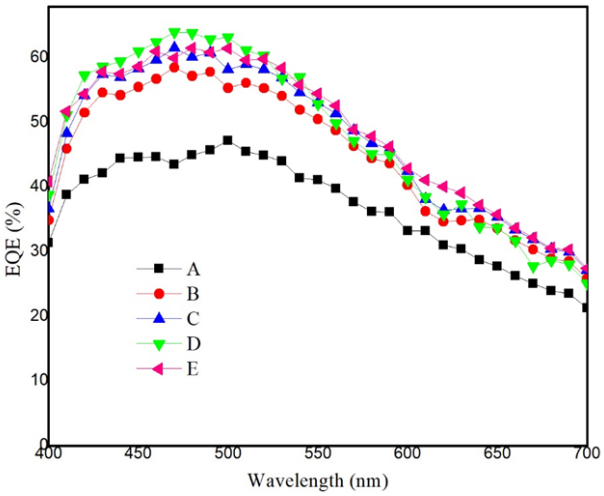

Fig. 6 – EQE of the hybrid solar cells: (A) without annealing and no NPs, (B) without annealing and with 0.05 mg Au NPs + 0.6 mg CuO NPs, (C) with 0.05 mg Au NPs + 0.6 mg CuO NPs and annealing at 150 °C, (D) with 0.05 mg Au NPs + 0.6 mg CuO NPs and annealing at 200 °C, (E) with 0.05 mg Au NPs + 0.6 mg CuO NPs and annealing at 250 °C

value was 64 %. This result shows that the EQE does not follow a similar pattern of results obtained from AFM analysis, XRD and UV-Vis spectroscopic data. This decreased EQE value of the sample annealed at 250 °C (device E) may be due to the agglomeration of Au and CuO NPs at higher temperature values.

The EQE improvements coincide with the J_{sc} and PCE enhancement of the devices. Fig. 7 exhibits the *J-V* characteristics of ITO/PEDOT:PSS/P3HT:PCBM:Au:CuO NPs/Al solar cells before and after thermal annealing treatment. Also, the *J-V* characteristic of the reference device (without annealing and without NPs in the active layer) was obtained for comparison purposes. The electrical parameters of all the devices are listed in Table 1. It is clear that J_{sc} increased from 5.838 to 6.790 mA/cm^2 by adding Au and CuO NPs in the active layer. Furthermore, J_{sc} increased to 8.114, 8.704 and 8.294 mA/cm^2 after annealing the devices at 150, 200 and 250 °C, respectively. The highest J_{sc} value (8.704 mA/cm^2) was exhibited by the PSC annealed at 200 °C. The FF values decreased from 58 to 55 %. However, the FF value remained unchanged at 56 % of the devices annealed at 200 and 250 °C. The FF explains the combination of the series (R_s) and shunt (R_{sh}) resistances of the device. R_s represents the sum of the contact resistance on the front/back surfaces and the ohmic resistances. Shunt resistance is mainly due to the imperfections on the device surface [25]. Au NPs and CuO NPs did not show a significant influence on the resistance of the device. However, thermal annealing decreased the FF of the devices as shown in Table 1 and it may be due to the increased NPs agglomeration after annealing. This clearly shows that the electrical parameter J_{sc} is improved significantly with thermal annealing treatment. However, before annealing the V_{oc} of all fabricated solar cells was almost a constant value around 0.65V. The V_{oc} values were slightly enhanced to 0.67 V after thermal annealing. The V_{oc} of PSCs depends on the energy difference between the highest occupied molecular orbital (HOMO) level of the donor (P3HT) and the lowest unoccupied molecular orbital (LUMO) level of the receptor (PCBM). This study reveals that the energy difference between the HOMO and LUMO levels of P3HT and PCBM remains unchanged under the annealing treatment at different temperature values. However, it can be slightly improved compared to the devices with and without the inclusion of Au/CuO NPs. Subsequently, the improved J_{sc}, UV absorption, EQE, FF and morphology enhanced the PCE from 2.201 to 3.266 %.

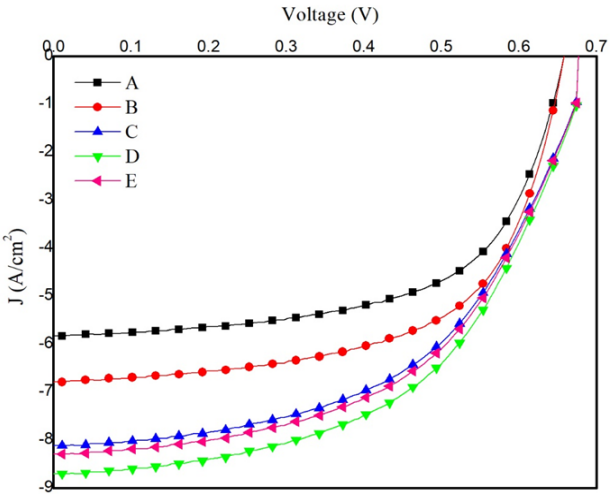

Fig. 7 – *J-V* characteristics of the hybrid solar cells: (A) without annealing and no NPs, (B) without annealing and with 0.05 mg Au NPs + 0.6 mg CuO NPs, (C) with 0.05 mg Au NPs + 0.6 mg CuO NPs and annealing at 150 °C, (D) with 0.05 mg Au NPs + 0.6 mg CuO NPs and annealing at 200 °C, (E) with 0.05 mg Au NPs + 0.6 mg CuO NPs and annealing at 250 °C

Table 1 – Performance parameters of the hybrid solar cells: (A) without annealing and no NPs, (B) without annealing and with 0.05 mg Au NPs + 0.6 mg CuO NPs, (C) with 0.05 mg Au NPs + 0.6 mg CuO NPs and annealing at 150 °C, (D) with 0.05 mg Au NPs + 0.6 mg CuO NPs and annealing at 200 °C, (E) with 0.05 mg Au NPs + 0.6 mg CuO NPs and annealing at 250 °C

Sample	J_{sc} (mA/cm^2)	V_{oc} (V)	FF (%)	PCE (%)
A	5.838	0.65	58	2.201
B	6.790	0.65	58	2.559
C	8.114	0.68	55	3.035
D	8.704	0.67	56	3.266
E	8.294	0.67	56	3.112

4. CONCLUSIONS

In this study, both Au and CuO NPs were added to the P3HT/PCBM layer of the solar cells, and these devices were annealed at three different temperatures (150, 200 and 250 °C) to increase the PCE. The PCE increased from 2.201 to 3.266 % in the cells annealed at 200 °C, which is equivalent to 48.3 % improvement in efficiency. The higher performance is attributed to enhanced UV-Vis absorption, EQE, J_{sc} and surface morphology.

The optical absorption spectrum changed significantly after the presence of Au NPs in the P3HT/PCBM active layer due to the strong field in the near zone around Au NPs. EQE of the solar cells increased due to increased hole and electron polaron mobilities in the cells and increased P3HT crystallinity. AFM analysis showed improved surface roughness of the P3HT/PCBM active layer. Thermal annealing significantly contributed to enhance UV-Vis absorption, EQE, J_{sc} and surface morphology including P3HT crystallinity. Also, SEM showed the uniformity of the annealed P3HT/PCBM/Au/CuO NPs active layer.

REFERENCES

1. R. Raja, W.S. Liu, C.Y. Hsiow, S.P. Rwei, W.Y. Chiu, L. Wang, *J. Mater. Chem. A* **3**, 14401 (2015).
2. C. Deibel, V. Dyakonov, *Rep. Prog. Phys.* **73**, 096401 (2010).
3. S. Gunes, H. Neugebauer, N.S. Sariciftci, *Chem. Rev.* **107**, 1324 (2007).
4. A.P. Wanninayake, S. Gunashekar, S. Li, B. Church, N. Abu-Zahra, *J. Sol. Energy Eng.* **137**, 031016 (2015).
5. B. Kan, H. Feng, H. Yao, M. Chang, X. Wan, C. Li, J. Hou, Y.A. Chen, *Sci. China Chem.* **61**, 1307 (2018).
6. Z. Xiao, X. Jia, L. Ding, *Sci. Bull.* **62**, 1562 (2017).
7. H. Zhang, H. Yao, J. Hou, J. Zhu, J. Zhang, W. Li, R. Yu, B. Gao, S. Zhang, J. Hou, *Adv. Mater.* **30**, 1800613 (2018).
8. L. Meng, Y. Zhang, X. Wan, C. Li, X. Zhang, Y. Wang, X. Ke, Z. Xiao, L. Ding, R. Xia, H. Yip, Y. Cao, Y. Chen, *Science* **361**, 1094 (2018).
9. M. Campoy-Quiles, T. Ferenczi, T. Agostinelli, P.G. Etchegoin, Y. Kim, T.D. Anthopoulos, P.N. Stavrinou, D.D.C. Bradley, J. Nelson, *Nat. Mater.* **7**, 158 (2008).
10. V. Shrotriya, Y. Yao, G. Li, Y. Yang, *Appl. Phys. Lett.* **89**, 063505 (2006).
11. A. Tabrizi, F. Ayhan, H. Ayhan, *Hacettepe J. Biol. Chem.* **37**, 217 (2009).
12. G. Li, V. Shrotriya, Y. Yao, Y. Yang, *J. Appl. Phys.* **98**, 043704 (2005).
13. D.D.S. Fung, L.F. Qiao, W.C.H. Choy, C. Wang, W.E.I. Sha, F. Xie, S. He, *J. Mater. Chem.* **21**, 16349 (2011).
14. H.A. Atwater, A. Polman, *Nat. Mater.* **9**, 205 (2010).
15. J.A. Schuller, E.S. Barnard, W. Cai, Y.C. Jun, J.S. White, M.L. Brongersma, *Nat. Mater.* **9**, 193 (2010).
16. M.D. Brown, T. Suteewong, R.S.S. Kumar, V.D. Innocenzo, A. Petrozza, M.M. Lee, U. Wiesner, H.J. Snaith, *Nano Lett.* **11**, 438 (2011).
17. L. Lu, Z. Luo, T. Xu, L. Yu, *Nano Lett.* **13**, 59 (2013).
18. Z. Yiwei, J.P. Andrew, F. Pontecchiani, J.F.K. Cooper, R.L. Thompson, R.A.L. Jones, S.M. King, D.G. Lidzey, G. Bernardo, *Sci. Rep.* **7**, 44269 (2017).
19. N.R. Dhineshbabu, V. Rajendran, N. Nithyavathy, R. Vetumperumal, *Appl. Nanosci.* **6**, 933 (2016).
20. E. Salim, S.R. Bobbara, A. Oraby, J.M. Nunzi, *Synth. Met.* **252**, 21 (2019).
21. G. Li, V. Shrotriya, Y. Yao, Y. Yang, *J. Appl. Phys.* **98**, 043704 (2005).
22. T.L. Wang, Y.T. Shieh, C.H. Yang, T.H. Ho, C.H. Chen, *Express Polym. Lett.* **7**, 63 (2013).
23. J. Park, J.E. Royer, C.N. Colesniuc, F.I. Bohrer, A. Sharoni, S. Jin, I.K. Schuller, W.C. Trogler, A.C. Kummel, *J. Appl. Phys.* **106**, 034505 (2009).
24. K. Kim, D.L. Carroll, *Appl. Phys. Lett.* **87**, 203113 (2005).
25. J. Zhang, S.T. Lee, B. Sun, *Electrochim. Acta* **146**, 845 (2014).

Вплив відпалу на оптоелектронні характеристики сонячних елементів P3HT/PCBM, що містять наночастинки Au і CuO

Aruna P. Wanninayake

Department of Physics and Electronics, University of Kelaniya, Kelaniya, Sri Lanka

Перетворення сонячної енергії в електричну за допомогою наноструктурованих органічних/неорганічних гібридних напівпровідників є одним з найкращих рішень сьогоднішньої енергетичної кризи. Зокрема, дослідники зосереджуються на мультитехніках для підвищення ефективності перетворення енергії полімерних сонячних елементів, включаючи термічний відпал та додавання наночастинок (NPs) оксиду металу або перехідного металу в активний шар полімерних сонячних елементів (PSCs). Конструктивні підходи до термічного відпалу спрямовані на покращення нанорозмірної морфології та оптичних властивостей активного шару. Впровадження металевих NPs базується на ефекті локалізованого поверхневого плазмонного резонансу (LSPR), який може бути використаний для посилення оптичного поглинання у фотоелектричних приладах. Тим часом NPs перехідного металу, такі як NPs оксиду міді (CuO) в активному шарі, відіграють ключову роль як центри акумулювання світлової енергії, центри стрибків заряджених частинок і проявники морфології поверхні, що дозволяє значно зменшити фізичну товщину шарів, які поглинають сонячну енергію. У дослідженні термічний відпал було використано для оптимізації ефективності перетворення енергії PSCs з об'ємними гетеропереходами P3HT/PC70BM, синтезованих шляхом включення наночастинок золота та наночастинок оксиду міді. Тепловий відпал збільшив ефективність перетворення енергії PSCs до 48,3 % порівняно з еталонним елементом. Оптимальна густина струму короткого замикання (J_{sc}) елементів склала 8,704 мА/см^2 порівняно із густиною 5,838 мА/см^2 в еталонному елементі; тим часом зовнішня квантова ефективність (EQE) зросла з 44 до 64 %.

Ключові слова: Плазмонний ефект, Термічний відпал, PSCs, P3HT, PCBM, PCE.